

Cosmological Constraints from Type Ia Supernovae Peculiar Velocity Measurements

C. Gordon, K. Land, and A. Slosar
Oxford Astrophysics, Physics, DWB, Keble Road, Oxford, OX1 3RH, UK

We detect the correlated peculiar velocities of nearby type Ia supernovae (SNe), while highlighting an error in some of the literature. We find $\sigma_8 = 0.79 \pm 0.22$ from SNe alone, and examine the potential of this method to constrain cosmological parameters in the future. We demonstrate that a survey of 300 low- z SNe (such as the nearby SNfactory) will underestimate constraints on w by $\sim 35\%$ if the coherent peculiar velocities are not included.

The first compelling evidence that the Universe was undergoing a period of accelerated expansion was provided by observations of Type Ia supernovae (SNe) [1, 2]. The data from many current [3–5] and near future [6–9] surveys should eventually constrain the effective dark energy equation of state to better than 10%.

Density inhomogeneities cause the SNe to deviate from the Hubble flow, as gravitational instability leads to matter flowing out of under-densities and into over-densities. These “peculiar velocities” (PVs) lead to an increased scatter in the Hubble diagram, of which several studies have been made [10–19]. When combining low and high redshift SNe in order to estimate the properties of the dark energy, the velocity contributions are usually modeled as a Gaussian noise term which is uncorrelated between different SNe. However, as recently emphasized [20], in the limit of low redshift $z \lesssim 0.1$ and large sample size, the correlations between SNe PVs contribute significantly to the overall error budget.

In this letter we investigate the effect of incorporating these correlations using the largest available low redshift compilation [17]. In Sec. I we outline how the PV covariances depend on the matter power spectrum. This formalism is then applied to the current data in Sec. II, where we detect the correlations at over the 3σ level. In Sec. III we look at future surveys and find that constraints on parameters such as w will be significantly underestimated if PVs are not accounted for.

I. PECULIAR VELOCITY COVARIANCE

The luminosity distance, d_L , to a SN at redshift z , is defined such that $\mathcal{F} = \frac{\mathcal{L}}{4\pi d_L^2}$ where \mathcal{F} is the observed flux and \mathcal{L} is the SN’s intrinsic luminosity. Astronomers use magnitudes, which are related to the luminosity distance (in megaparsec) by $\mu \equiv m - M = 5 \log d_L + 25$, where m and M are the apparent and absolute magnitudes respectively. In the context of SNe, M is a “nuisance parameter” which is degenerate with $\log(H_0)$ and can be marginalised over. For a Friedmann-Robertson-Walker Universe the predicted luminosity distance is given by

$$d_L(z) = (1+z) \int_0^z \frac{dz'}{H(z')} \quad (1)$$

in speed of light units, where H is the Hubble parameter. In the limit of low redshift this reduces to $d_L \approx z/H_0$.

The effect of peculiar velocities is two-fold: the observed redshift is modified by a Doppler shift, and the observers motion leads to a distance dipole correction. Overall, these lead to a perturbation in the luminosity distance (δd_L) given by [20–24]

$$\frac{\delta d_L}{d_L} = \hat{\mathbf{r}} \cdot \left(\mathbf{v} - \frac{(1+z)^2}{H(z) d_L} [\mathbf{v} - \mathbf{v}_O] \right) \quad (2)$$

where \mathbf{r} is the position of the SN, and \mathbf{v}_O and \mathbf{v} are the peculiar velocities of the observer and SN respectively. Using the Cosmic Microwave Background dipole we can very accurately correct for \mathbf{v}_O . This demonstrates how a SNe survey that measures μ and z can estimate the projected PV field. We now relate this to the cosmology.

The statistical distribution of the velocities, $\xi(\mathbf{r}_i, \mathbf{r}_j) \equiv \langle (\mathbf{v}(\mathbf{r}_i) \cdot \hat{\mathbf{r}}_i)(\mathbf{v}(\mathbf{r}_j) \cdot \hat{\mathbf{r}}_j) \rangle$, must be rotationally invariant, and therefore is can be decomposed into a parallel and perpendicular components [25–27] :

$$\xi(\mathbf{r}_i, \mathbf{r}_j) = \sin \theta_i \sin \theta_j \xi_{\perp}(r, z_i, z_j) + \cos \theta_i \cos \theta_j \xi_{\parallel}(r, z_i, z_j)$$

where $\mathbf{r}_{ij} \equiv \mathbf{r}_i - \mathbf{r}_j$, $r = |\mathbf{r}_{ij}|$, $\cos \theta_i \equiv \hat{\mathbf{r}}_i \cdot \hat{\mathbf{r}}_{ij}$, and $\cos \theta_j \equiv \hat{\mathbf{r}}_j \cdot \hat{\mathbf{r}}_{ij}$. In linear theory, these are given by [25–27]:

$$\xi_{\parallel, \perp} = D'(z_i) D'(z_j) \int_0^\infty \frac{dk}{2\pi^2} P(k) K_{\parallel, \perp}(kr) \quad (3)$$

where $K_{\parallel}(x) = j_0(x) - \frac{2j_1(x)}{x}$, $K_{\perp}(x) = j_1(x)/x$. $D(z)$ is the growth function, and derivatives are with respect to conformal time. $P(k)$ is the matter power spectrum. This corrects the formulae used in [28, 29], see the Appendix for details.

The above estimate of $\xi(\mathbf{r}_i, \mathbf{r}_j)$ is based on linear theory. The small scale nonlinear contribution (σ_v) is usually modeled as an uncorrelated term which is independent of redshift, often set to ~ 300 km/s. Other random errors that are usually considered are those from the lightcurve fitting (μ_{err}), and some intrinsic magnitude scatter (σ_m) found to be ~ 0.08 in the case of [17]. It is just these three errors that are usually included in the analysis of SNe.

In Fig. 1 we compare the covariance from peculiar velocities for a pair of SN

$$C_v(i, j) = \left(1 - \frac{(1+z)^2}{H d_L} \right)_i \left(1 - \frac{(1+z)^2}{H d_L} \right)_j \xi(\mathbf{r}_i, \mathbf{r}_j), \quad (4)$$

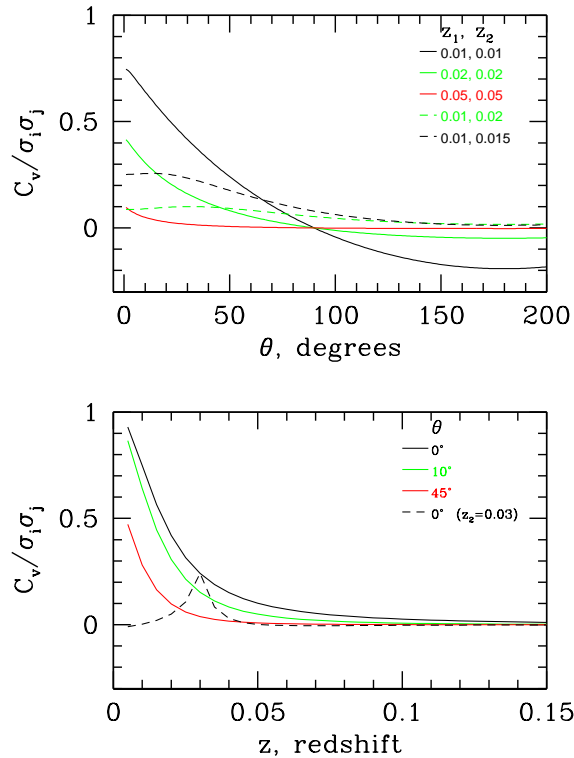


FIG. 1: The ratio of the covariance from peculiar velocities C_v , compared to the random errors σ , for a pair of supernovae, over a range of separations. In the upper panel we vary the separation on the sky, θ . In the lower panel we vary the redshift, with them both at the same z (solid lines) or with one supernovae fixed at $z = 0.03$ (dashed).

to the standard random errors σ (consisting of $\mu_{err} = 0.1$, $\sigma_m = 0.08$, and $\sigma_v = 300$ km/s added together in quadrature). We see that the PV covariance is comparable with the random errors for low- z , and we note that these correlated errors become more significant the larger the dataset.

II. CONSTRAINTS FROM CURRENT DATA

A random-error-only analysis of SNe allows one to constrain the cosmological parameters through the Hubble parameter in (1). Namely Ω_m and w , for a flat Universe. However, by fitting for the PV covariance we probe the matter power spectrum and can therefore constrain further parameters such as Ω_b , H_0 , n_s , σ_8 , where these have their usual meaning. In the following analysis we also allow the SNe “nuisance” parameters M , σ_m , σ_v to vary. These are often set to fixed values, however marginalizing over them allows a better estimate of the uncertainty in the other parameters. The likelihood is only weakly sensitive to Ω_b , n_s , and H_0 , as the power spectrum on the scales relevant to the PVs depends mainly on σ_8 and to a lesser extent on Ω_m .

We analyse nearby supernovae ($z \leq 0.12$) from [17]

who find improved luminosity distances to 133 supernovae from a multicolour light curve method. Following [17] we exclude 9 supernovae from the set. These are supernovae that are unsuitable due to bad lightcurve fits, those who have their first observation more than 20 days after maximum light, are hosted in galaxies with excessive extinction ($A_V^0 > 2.0$ mag) and one outlier (SN1999e). This leaves 124 supernovae $z \in [0.0023, 0.12]$, which have an average separation of $\bar{r} = 108 h^{-1}$ Mpc, a mean redshift $\bar{z} = 0.024$, and herein we refer to this dataset as our “low- z ” SNe.

We assume a flat Universe with a cosmological constant ($w = -1$), a Big Bang Nucleosynthesis (BBN) prior $\Omega_b h^2 \sim \mathcal{N}(0.0214, 0.002)$ [30], and a Hubble Space Telescope (HST) prior $h \sim \mathcal{N}(0.72, 0.08)$ [31]. These two priors remove models that are wildly at odds with standard cosmological probes, but do not unduly bias results towards standard cosmology. The likelihood has almost negligible dependence on n_s , and to keep it in a range consistent with CMB and large scale structure estimates we give it a uniform prior $n \in [-0.9, 1.1]$. The other parameters are all given broad uniform priors. We use the standard Markov Chain Monte Carlo (MCMC) method to generate samples from the posterior distribution of the parameters [32]. Convergence was checked using multiple chains with different starting positions, and also the $R-1$ statistic [33]. We also checked that the estimated posterior distributions reduced to the prior distributions when no data was used [36]. All the analysis was checked with two completely independent codes and MCMC chains.

The low- z results are given in row A of Table I. We also perform the MCMC runs without including the PV covariance matrix C_v , and we find $-2 \ln \mathcal{L}_{\max}$ (where \mathcal{L} is the likelihood) increases by 19.3. As the likelihood no longer depends on $\{\sigma_8, \Omega_b, h, n_s\}$ we have effectively removed four parameters. From the MCMC samples we estimate the mean of σ_8 to be 0.79 and its standard deviation to be 0.23, and thus σ_8 is between three and four standard deviations away from zero.

When estimating the cosmological parameters from SNe, a low redshift cut is usually imposed, to reduce the effects of the PVs. For example in [34], their SNe dataset have $z \in [0.016, 1.76]$ and a mean redshift of $\bar{z} = 0.48$. Herein we refer to this dataset as our “high- z ” SNe. Our MCMC results for just this data (without including PVs) are shown in row B of Table I. Although we marginalize over the SNe parameters $\{M, \sigma_v, \sigma_s\}$, our constraints on Ω_m are still in excellent agreement with those obtained in [34].

We now combine the low- z and the high- z datasets, to make an “all- z ” dataset. We used the overlapping SNe in the two datasets to estimate a small normalizing offset to the magnitudes from the latter data set, (the extra magnitude error is negligibly small). The same procedure was used by [34] in constructing their dataset. After eliminating duplicated SNe, our combined all- z dataset has 271 SNe with $z \in [0.0023, 1.76]$, and $\bar{z} = 0.35$. Our all- z results are given in row C of Table I. The constraints

	w	σ_8	Ω_m	σ_v	σ_m
A) low- z +PV+BBN+HST	-1	$0.79^{+0.22}_{-0.22}$	$0.48^{+0.30}_{-0.29}$	275^{+69}_{-70}	$0.08^{+0.03}_{-0.04}$
B) high- z	-1		$0.27^{+0.03}_{-0.03}$	363^{+169}_{-185}	$0.12^{+0.02}_{-0.02}$
C) all- z +PV+BBN+HST	-1	$0.78^{+0.23}_{-0.23}$	$0.30^{+0.04}_{-0.04}$	$301^{+53.9}_{-53.4}$	$0.1^{+0.02}_{-0.02}$
D) high- z +WMAP	$-0.96^{+0.09}_{-0.09}$	$0.76^{+0.07}_{-0.07}$	$0.26^{+0.03}_{-0.03}$	191^{+97}_{-104}	$0.10^{+0.02}_{-0.02}$
E) high- z +PV+WMAP	$-0.94^{+0.08}_{-0.08}$	$0.75^{+0.06}_{-0.06}$	$0.26^{+0.02}_{-0.03}$	149^{+107}_{-108}	$0.11^{+0.02}_{-0.02}$
F) all- z +WMAP	$-0.93^{+0.07}_{-0.07}$	$0.75^{+0.06}_{-0.07}$	$0.26^{+0.02}_{-0.02}$	395^{+42}_{-42}	$0.11^{+0.02}_{-0.02}$
G) all- z +PV+WMAP	$-0.86^{+0.08}_{-0.08}$	$0.72^{+0.06}_{-0.07}$	$0.28^{+0.03}_{-0.03}$	292^{+44}_{-45}	$0.11^{+0.02}_{-0.02}$
H) WMAP only	$-0.99^{+0.22}_{-0.22}$	$0.76^{+0.09}_{-0.09}$	$0.25^{+0.05}_{-0.05}$		

TABLE I: Mean and 68% confidence limits on the cosmological parameters, and σ_v, σ_m , using different combinations of the WMAP and SNe datasets, with and without including the peculiar velocity covariance matrix (PV). See text for discussion.

on σ_8 broaden slightly due to a mild degeneracy between σ_8 and Ω_m which is broken by the addition of the higher z SNe, but pushes σ_8 to the region of higher uncertainty. The increase in the minimum of $-2 \ln \mathcal{L}$, when σ_8 is set to zero, is now 16.4. The mean and standard deviation of σ_8 is 0.78 and 0.24. Therefore, the mean of σ_8 is still between three and four sigma away from zero.

One the main aims of cosmology is to test the cosmological constant prediction $w = -1$. Due to a degeneracy between w and Ω_m , it is necessary to combine the SNe with another data source. Here we use the WMAP CMB data [35]. We continue to assume a flat Universe, and we now allow w to be a free parameter. The results are given in rows D to H of Table I and in Fig. 2. As can be seen by comparing rows D and E, if a redshift cutoff of $z \geq 0.016$ is made, then current data has a systematic error of $\delta w = 0.02$ when PVs are not included. This is several times smaller than the statistical error of $\delta w = 0.08$. However, comparing rows F and G, shows that if no redshift cutoff is made, neglecting the correlated PVs results in a systematic error of $\delta w = 0.07$ which is about as large as the statistical error.

III. FUTURE FORECASTS

We now consider the relevance of peculiar velocities to future supernovae surveys, using a Fisher matrix analysis. The Fisher (information) matrix probes the ability of an experiment to constrain parameters, by looking at the dependence of the likelihood: $F_{\alpha\beta} \equiv -\left\langle \frac{\partial^2 \mathcal{L}}{\partial p_\alpha \partial p_\beta} \right\rangle$

$$F_{\alpha\beta} = \mathbf{d}_{,\alpha} \mathbf{C}^{-1} \mathbf{d}^T,_{\beta} + \frac{1}{2} \text{Tr} (\mathbf{C}^{-1} \mathbf{C}_{,\alpha} \mathbf{C}^{-1} \mathbf{C}_{,\beta}) \quad (5)$$

Often the second term is ignored, however we find that this approximation is no longer valid when including PVs. Unmarginalised 1σ errors on parameter p_α are given by $\sqrt{(1/F_{\alpha\alpha})}$, and the equivalent marginalised errors by $\sqrt{(\{F^{-1}\}_{\alpha\alpha})}$. Generally, the inverted Fisher matrix F^{-1} provides the expected covariance matrix for the parameters.

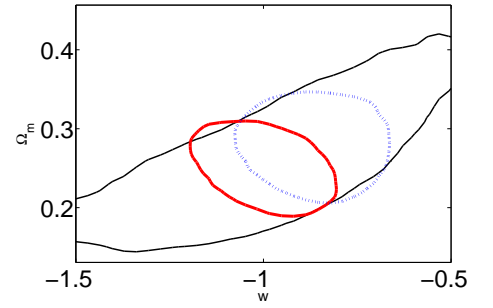


FIG. 2: 95% confidence limits on Ω_m and w , for WMAP only (thin black), WMAP with high- z SNe (thick red), and WMAP with all- z SNe including PVs (dotted blue)

We consider two future supernovae experiments that aim to detect high and low-redshift supernovae respectively: the Supernova/Acceleration Probe (SNAP, [9]), and the Nearby Supernova Factory (SNfactory, [6]). The baseline SNfactory program is to obtain spectrophotometric lightcurves for SNe in the redshift range $0.03 < z < 0.08$, with the assumption that these SNe are far enough away for galaxy peculiar velocities to not contribute significantly to the error budget. In Fig 1 we can see the contribution of PVs is not irrelevant for $z \sim 0.03$, and as the number of SNe increases the overall uncertainty from random errors (such as intrinsic magnitude scatter and instrumental noise) gets beaten down by a $1/\sqrt{N}$ factor, while the correlated errors from coherent peculiar velocities do not. Thus at any redshift, these peculiar velocity errors will begin to dominate for some large number of SNe. We investigate the situation for the SNfactory by considering 300 SNe randomly distributed over a rectangular area of 10,000 sq degrees, and redshifts $0.03 < z < 0.08$. We also include high- z from a SNAP-like survey, and model this as 2000 SNe randomly distributed over 10 sq degrees with $0.2 < z < 1.7$, and we assume PVs are irrelevant for these SNe. We take our fiducial model to be a flat Λ CDM cosmology with $\Omega_m=0.3$, $\Omega_b = 0.05$, $h = 0.7$, $n_s = 0.96$, $w = -1$, $\sigma_8 = 0.85$, and nuisance parameters $\sigma_v = 300$ km/s, $\sigma_m=0.1$, $\mu_{err} = 0.1$. We further marginalise over M .

In Fig 3 we compare the marginalised 1σ contours obtained when the coherent PVs are ignored and included, for our hypothetical SNAP and SNfactory surveys. We see that, even for a cut of $z > 0.03$ the error bars on Ω_m and w will be considerably underestimated if the peculiar velocities are ignored, and in particular the marginalised error on w increases from 0.062 to 0.084, for the SNe alone. We therefore conclude that it is essential to include a full covariance matrix analysis at these redshifts, to avoid significantly underestimating the errors. That the error bars increase rather than decrease indicates that the extra information available in the peculiar velocities is outweighed by the extra parameter space $\{\Omega_b, h, n_s, \sigma_8\}$.

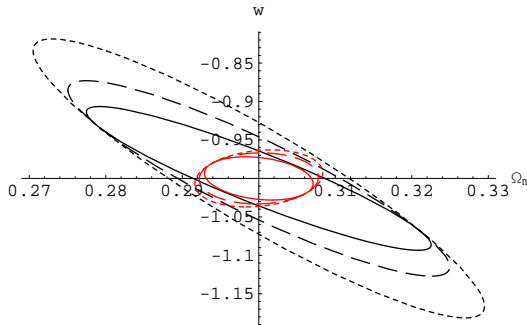


FIG. 3: The marginalised 1σ contours for Ω_m and w from a SNAP-like high- z SNe survey in a flat Λ CDM cosmology (short dashed lines). We also consider including 300 low- z SNe from a SNfactory-like survey, while ignoring peculiar velocities (solid lines) and including them (long dashed lines). Smaller red contours include cosmic variance limited CMB, up to $\ell = 2000$.

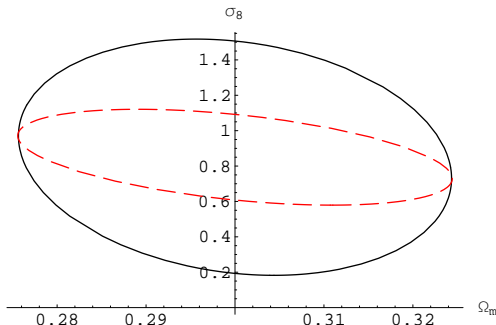


FIG. 4: The marginalised 1σ contours for Ω_m and σ_8 , from 1000 low- z SNe in a Λ CDM cosmology, with $0.03 < z < 0.08$ (black solid line) and $z < 0.08$ (red dashed line), combined with a SNAP-like high- z SNe survey.

In light of the extra effort required for the low- z SNe we consider excluding them. However in Fig 3 we see that the contours increase significantly when low- z SNe are not available (marginalised error on w increase to 0.12), even when CMB data is included. Therefore we conclude that low- z SNe play a vital role in constraining the cosmological parameters, but a full covariance matrix analysis must be done.

We have shown that a low redshift cut of 0.03 is futile in avoiding peculiar velocities when we have 100's of SNe. We therefore consider that no lower bound on redshift is needed at all, and we extend our study to include SNe with $z < 0.03$. We consider a survey of 1000 SNe randomly distributed over 10,000 sq degrees and redshifts

$z < 0.08$, and compare it to a similar survey of 1000 SNe, but with $0.03 < z < 0.08$. We combine them with a high- z SNAP-like survey as above. In Fig 4 we see that by including very low- z SNe ($z < 0.03$) we have gained free information about σ_8 - 'free' because the error bars on Ω_m (and w) stay the same.

In summary, we have found that when no redshift cut-off is imposed, the current SNe data detects correlations in PVs at greater than the three sigma level. We also found that the current constraints on w are not sensitive to the the PVs if SNe with $z < 0.016$ are excluded. However, we have shown that future large scale data sets will be sensitive to the PVs even if a lower bound of $z \geq 0.03$ is used.

Appendix

For perturbations, $\rho(1 + \delta)$, and peculiar velocity \mathbf{v} we find the perturbed Fourier space continuity equation, in co-moving coordinates, is

$$\delta'_{\mathbf{k}} - i\mathbf{k} \cdot \mathbf{v}_{\mathbf{k}} = 0 \quad (\text{A1})$$

where prime indicates differentiation with respect to conformal time, η . Using the linear approximation $\delta_{\mathbf{k}}(\eta) = D(\eta)\tilde{\delta}_{\mathbf{k}}$, and assuming that the Universe has no vorticity ($\nabla \times \mathbf{v} = 0$) leads to

$$\mathbf{v}_{\mathbf{k}} = v_{\mathbf{k}} \hat{\mathbf{k}} = -iD' \frac{\tilde{\delta}_{\mathbf{k}}}{k^2} \mathbf{k}, \quad (\text{A2})$$

where $D(z)$ is the growth function. Therefore, the Fourier space correlation between the i th component of the velocity field at time η_A and the j th component of the velocity field at time η_B is given by

$$\left\langle v_{\mathbf{k}_A}^i v_{\mathbf{k}_B}^{j*} \right\rangle = D'(\eta_A)D'(\eta_B)(2\pi)^3 \delta(\mathbf{k}_A - \mathbf{k}_B) P(k_A) \frac{k_A^i k_A^j}{(k_A)^4}, \quad (\text{A3})$$

where $\langle \delta_{\mathbf{k}_A} \delta_{\mathbf{k}_B} \rangle = (2\pi)^3 \delta(\mathbf{k}_A - \mathbf{k}_B) P(k_A)$, and the subscripts denote the quantity at time η_A or η_B . This corrects equation (B1) of [28], and the resulting equations for C_v (4) correct those of [29], among others.

We thank Joe Silk, Pedro Ferreira, and Uroš Seljak for useful conversations. CG is funded by the Beecroft Institute of Particle Astrophysics and Cosmology, KRL by Glassstone research fellowship and Christ Church college, AS by Oxford Astrophysics. Results were computed on the UK-CCC COSMOS supercomputer.

[1] A. G. Riess et al. (Supernova Search Team), *Astron. J.* **116**, 1009 (1998), [astro-ph/9805201](#).
[2] S. Perlmutter et al. (Supernova Cosmology Project), *Astrophys. J.* **517**, 565 (1999), [astro-ph/9812133](#).
[3] P. Astier et al., *Astron. Astrophys.* **447**, 31 (2006), [astro-ph/0510447](#).
[4] A. G. Riess et al. (2006), [astro-ph/0611572](#).
[5] W. M. Wood-Vasey et al. (2007), [astro-ph/0701041](#).

- [6] G. Aldering et al., in *Survey and Other Telescope Technologies and Discoveries*, edited by J. A. Tyson and S. Wolff (2002), vol. 4836, pp. 61–72.
- [7] B. Dilday et al., in *Bulletin of the American Astronomical Society* (2005), vol. 37, pp. 1459–+.
- [8] M. Hamuy et al. (2005), astro-ph/0512039.
- [9] G. Aldering, *New Astron. Rev.* **49**, 346 (2005), astro-ph/0507426.
- [10] A. G. Riess, W. H. Press, and R. P. Kirshner, *Astrophys. J.* **445**, L91 (1995), astro-ph/9412017.
- [11] A. G. Riess, M. Davis, J. Baker, and R. P. Kirshner (1997), astro-ph/9707261.
- [12] I. Zehavi, A. G. Riess, R. P. Kirshner, and A. Dekel, *Astrophys. J.* **503**, 483 (1998), astro-ph/9802252.
- [13] A. Bonacic, R. A. Schommer, N. B. Suntzeff, and M. M. Phillips, *Bulletin of the American Astronomical Society* **32**, 1285 (2000).
- [14] D. J. Radburn-Smith, J. R. Lucey, and M. J. Hudson (2004), astro-ph/0409551.
- [15] C. Bonvin, R. Durrer, and M. Kunz, *Phys. Rev. Lett.* **96**, 191302 (2006), astro-ph/0603240.
- [16] T. Haugboelle et al. (2006), astro-ph/0612137.
- [17] S. Jha, A. G. Riess, and R. P. Kirshner, *Astrophys. J.* **659**, 122 (2007), astro-ph/0612666.
- [18] R. Watkins and H. A. Feldman (2007), astro-ph/0702751.
- [19] S. Hannestad, T. Haugboelle, and B. Thomsen (2007), arXiv:0705.0979 [astro-ph].
- [20] L. Hui and P. B. Greene, *Phys. Rev. D* **73**, 123526 (2006), astro-ph/0512159.
- [21] M. Sasaki, *Mon. Not. Roy. Astron. Soc.* **228**, 653 (1987).
- [22] N. Sugiura, N. Sugiyama, and M. Sasaki, *Progress of Theoretical Physics* **101**, 903 (1999).
- [23] T. Pyne and M. Birkishaw, *Mon. Not. Roy. Astron. Soc.* **348**, 581 (2004), astro-ph/0310841.
- [24] C. Bonvin, R. Durrer, and M. A. Gasparini, *Phys. Rev. D* **73**, 023523 (2006), astro-ph/0511183.
- [25] K. Gorski, *Astrophys. J.* **332**, L7 (1988).
- [26] E. J. Groth, R. Juszkiewicz, and J. P. Ostriker, *Astrophys. J.* **346**, 558 (1989).
- [27] S. Dodelson, *Modern cosmology* (Academic Press, 2003).
- [28] C. Hernandez-Monteagudo, L. Verde, R. Jimenez, and D. N. Spergel, *Astrophys. J.* **643**, 598 (2006), astro-ph/0511061.
- [29] A. Cooray and R. R. Caldwell, *Phys. Rev. D* **73**, 103002 (2006), astro-ph/0601377.
- [30] D. Kirkman, D. Tytler, N. Suzuki, J. M. O’Meara, and D. Lubin, *Astrophys. J. Suppl.* **149**, 1 (2003), astro-ph/0302006.
- [31] W. L. Freedman et al., *Astrophys. J.* **553**, 47 (2001), astro-ph/0012376.
- [32] A. Lewis and S. Bridle, *Phys. Rev. D* **66**, 103511 (2002).
- [33] A. Gelman and D. Rubin, *Stat. Sci.* **7**, 457 (1992).
- [34] T. M. Davis et al. (2007), astro-ph/0701510.
- [35] D. N. Spergel et al. (WMAP) (2006), astro-ph/0603449.
- [36] We note that when only weak data are present, the implied priors can have significant effect. In particular, the default `cosmomc` parametrisation is not suitable for our work in absence of CMB or comparably constraining datasets.